NOx emissions reduction and rebound in China due to the COVID-19 crisis

J.Ding[1], R.J. van der A[1,2], H.J. Eskes[1], B. Mijling[1], T. Stavrakou[3], J.H.G.M. van Geffen[1], J.P. Veefkind[1,4]

[1] Royal Netherlands Meteorological Institute (KNMI), Utrechtseweg 297, 3731 GA De Bilt, The Nederlands.

[2] Nanjing University of Information Science & Technology (NUIST), Ningliu Road 219, Nanjing, P.R. China.

[3] Royal Belgian Institute for Space Aeronomy (BIRA-IASB), Avenue Circulaire 3, 1180 Brussels, Belgium.

[4] Delft University of Technology, Stevinweg 1, 2628 CN Delft, The Netherlands

Corresponding author: Jieying Ding (jieying.ding@knmi.nl)

Key Points:

- NO_x emissions derived from TROPOMI observations show reductions for individual Chinese cities of about 35% due to the COVID-19 lockdown.
- Emissions of coal power plants and maritime transport show strong reductions (25-40%) during the lockdown.
- Urban emissions rebound in March to levels before the lockdown, while emissions of power plants and maritime transport take longer to recover.

Abstract

During the COVID-19 lockdown (24 Jan to 20 March) in China low air pollution levels were reported in the media as a consequence of reduced economic and social activities. Quantification of the pollution reduction is not straightforward due to effects of transport, meteorology, and chemistry. We have analysed the NO_x emission reductions calculated with an inverse algorithm applied to daily NO_2 observations from TROPOMI onboard the Copernicus Sentinel-5P satellite. This method allows the quantification of emission reductions per city, and the analysis of emissions of maritime transport and of the energy sector separately. The reductions we found are 20 to 50% for cities, about 40% for power plants and 15 to 40% for maritime transport depending on the region. The reduction in both emissions and concentrations shows a similar timeline consisting of a sharp reduction (34 to 50%) around the Spring festival and a slow recovery from mid-February to mid-March.

Plain Language Summary

During the COVID-19 lockdown in China, air quality had strongly improved. Here we study what sources were reduced and how much the reduction per city was. We used TROPOMI observations of the Sentinel-5P satellite, which monitors the Earth's atmosphere daily. We focused on observations of the pollutant 'nitrogen dioxide', an important pre-cursor of air pollution in the atmosphere. With our novel methodology we are able to calculate the pollution back to the sources of the emissions, whether these are big cities, industrial regions, power plants or busy shipping lanes. We applied this method to East China, where the 36 biggest Chinese cities are located. Almost all those cities showed strong emission reductions of 20-50% during the lockdown in February 2020. Besides urban China, we found an average emission reduction of 40% over coal power plants, and a reduction in maritime transport by 15-40% depending on the region. The period of reduced emissions lasted until around the end of February and the emissions slowly returned to normal during the month March 2020. Exception is the region Wuhan, the centre of the COVID-19 crisis, where emissions started to rebound since 8 April, the end of their lockdown period.

1 Introduction

The year 2020 is an unprecedented year, with the novel coronavirus, causing the COVID-19 disease spreading over the whole world, infecting millions of people and causing hundreds of thousands of fatalities (WHO, 2020). On 11 March 2020, the World Health Organization (WHO) qualified the spread of COVID-19 as a pandemic. To prevent the spread of the disease, many affected countries implemented COVID-19 regulations. China, the first country facing the outbreak of COVID-19, enacted a lockdown from 24 January to 20 March 2020 in the Hubei province where the first cases were reported from its capital Wuhan, while other provinces limited all outdoor activities since the Chinese New Year and gradually resumed the work after 10 February (Tian et al., 2020; Wang et al., 2020).

The strict COVID-19 regulations lead to a reduction of road and air traffic, a temporary closing of companies and a decrease of industrial productivity. These in consequence affect emissions of air pollutants, especially from the transport and industry sectors, which are significant sources of NO_x (NO_x=NO_2+NO) in cities. Several studies presented a large decrease

of NO_2 concentration during the lockdown period in China from both in-situ and satellite observations (Wang et al., 2020; Huang et al., 2020). Tropospheric NO_2 column concentrations observed by the TROPOMI (TROPOspheric Monitoring Instrument) on the Sentinel-5P satellite decrease about 35% over China and some areas up to 60% during the COVID-19 regulation period compared to the same period of 2019 (Bauwens et al, 2020; Zhang et al., 2020; Liu et al., 2020). In March 2020, after the resumption of work and the gradual lifting of the lockdown restrictions, the NO_2 concentrations quickly increased to similar levels as in the previous year (Bauwens et al., 2020). Because NO_2 concentrations are affected by meteorology, chemistry and transport, large concentration variations are expected from day to day. Therefore the concentrations alone provide only an indication of the impact of the COVID-19 measures on air pollution. Bottom-up inventories are usually updated with few years delay due to the complexity of gathering all statistic information on source sector, land-use and sector-specific emission factors. A top-down approach using satellite observations has been demonstrated to be able to accurately and quickly provide emission estimates (Stavrakou et al., 2013; Miyazaki et al. 2020). Here we derived the NO_x emissions by using the satellite observations and a chemistry-transport model (CTM). The model is driven by meteorological analyses, accounting for the weather-related variability. The high spatial resolution of the TROPOMI observations and the inverse modelling system allows us to quantify the impact of the COVID-19 measures and distinguish emissions from cities, power plants and maritime transport separately. Recently, NO_x emissions derived from the high resolution NO_2 observations of TROPOMI have been reported by Goldberg et al. (2019) and van der A et al. (2020).

To this purpose, we use the DECSO (Daily Emission estimates Constrained by Satellite Observations) algorithm, which has been demonstrated to capture emission changes in a short time period at city level (Mijling and van der A, 2012; Ding et al., 2015). This study presents NO_x emissions estimated from Sentinel-5P TROPOMI observations from 2019 to April 2020 over East Asia. The high spatial resolution satellite observations and daily global coverage allow us to monitor fast emission changes per city due to the implementation and to the relaxing of COVID-19 regulations.

2 Methodology

2.1 NO_2 observations by TROPOMI

The Copernicus Sentinel-5P satellite carries the TROPOMI instrument (Veefkind et al, 2012). TROPOMI is a spectrometer combining a high spectral resolution with high spatial resolution (3.5 x 5.5 km^2 at nadir for the NO_2 observations), low noise and a daily global coverage. Despite the much smaller footprints, the spectral fits of the individual TROPOMI groud pixels have 30% smaller noise than those from the earlier Ozone Monitoring Instrument (OMI) and the average values agree well within 5% (van Geffen et al, 2020).

Validation studies (Judd et al, 2020; Tack et al, 2020; Verhoelst et al, 2020) show that the currently available TROPOMI product (versions 1.2.2 and 1.3.0) has tropospheric columns with effectively a typical systematic bias of about -15% (see Supplementary Information), and we expect the derived emissions from these observations to be low by such an amount on

average. In the relative comparisons discussed in this paper for both columns and emissions we expect a large part of such a multiplicative bias to cancel out.

Figure 1 (a and b) shows the mean TROPOMI NO_2 tropospheric column observations gridded on a 0.02^o by 0.02^o grid for the periods 8-28 February 2020 compared with 18 February to 4 March 2019, both after the Chinese New Year holidays. Very prominent concentration reductions are observed in 2020 compared to 2019.

The TROPOMI tropospheric NO_2 columns are pre-processed into "super-observations", representing the integrated average of the TROPOMI observations over the 0.25^o x 0.25^o grid cells of the model after filtering for clouds. The basic concept of super-observations has been explained in Myazaki et al. (2012) and Boersma et al. (2016). They have shown that clustering individual observations into super-observations has a positive impact on the analysis. The super-observation error takes into account spatial correlations between individual TROPOMI observations as well as representativity errors in the case of incomplete coverage. Averaging kernels are also computed for these super-observations, and are used in the emission estimates described below. This has the advantage that the inversion result becomes independent of the coarser-resolution of the a priori profile used in the retrieval of the tropospheric column.

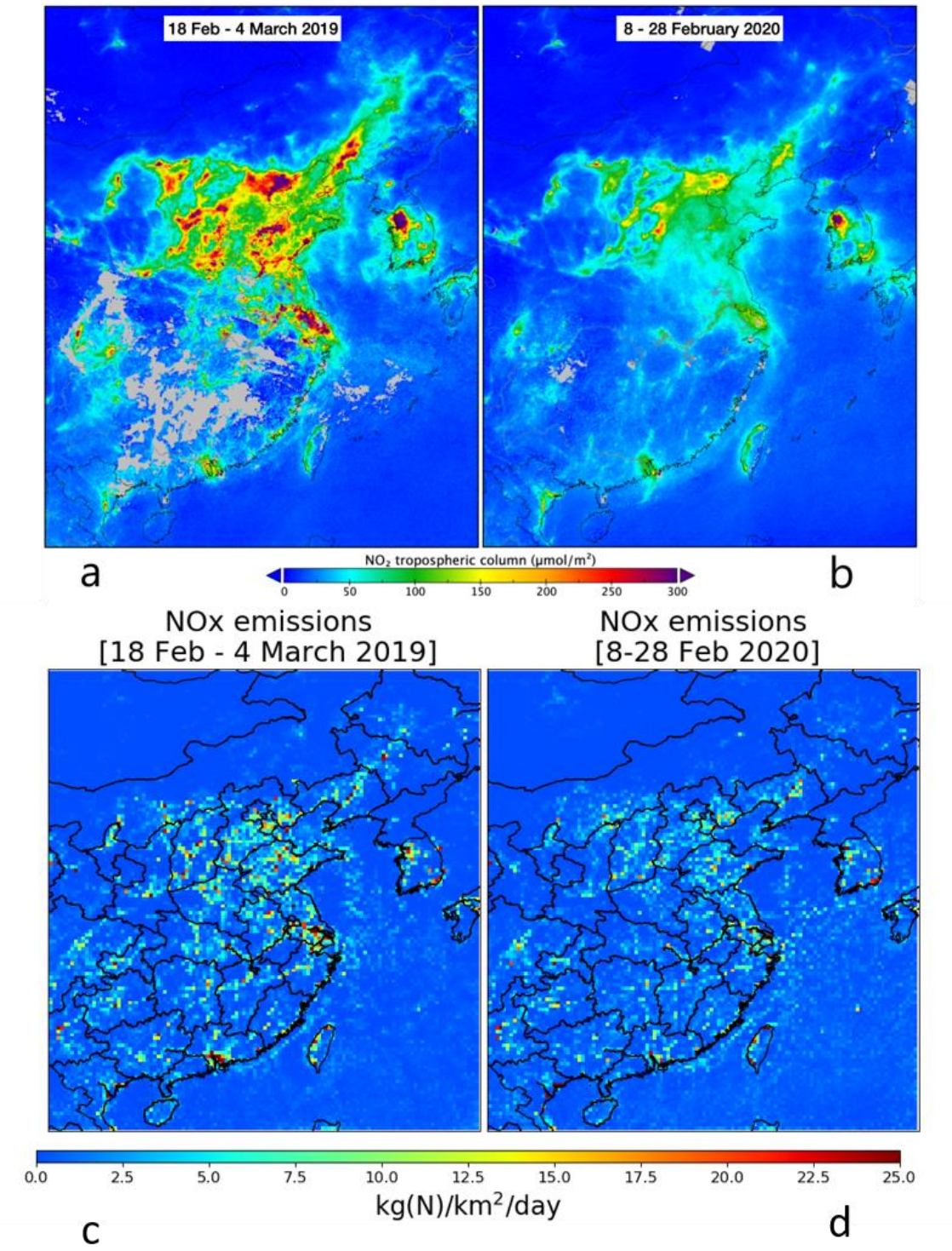

Figure 1. TROPOMI NO_2 columns over East China after the Chinese New Year in 2019 (a) and 2020 (b). NO_x emissions for the same period in 2019 (c) and 2020 (d) derived with DECSO.

2.2 NO_x emissions from DECSO

DECSO is a state-of-the-art inverse algorithm developed by Mijling and van der A (2012) to update daily emissions of short-lived atmospheric constituents using an extended Kalman filter, in which emissions are translated to concentrations via a CTM and compared to the satellite observations. The sensitivity of concentrations to emissions is calculated from a trajectory analysis to account for transport of the short-lived gas by using a single CTM forward run. DECSO has been successfully applied to NO_2 observations from OMI and TROPOMI over different regions (Mijling and van der A, 2012; Ding et al., 2017, 2018; van der A et al., 2020). In this study, daily NO_x emissions from January 2019 to April 2020 over East Asia (102–120°E, 18–50°N) are derived with DECSO using the Eulerian regional off-line CTM CHIMERE v2013 (Menut et al., 2013) and TROPOMI NO_2 observations. The implementation of CHIMERE v2013 in DECSO is described in Ding et al. (2015). The latest development and validation of DECSO are presented in previous studies (Ding et al., 2017; van der A et al., 2020). In our current approach, we apply DECSO to the super-observations of TROPOMI instead of directly using individual TROPOMI observations. Figure 1 (c and d) shows the mean NOx emissions derived from TROPOMI for the same period as Figure 1a and 1b in 2019 and 2020 after the Chinese New Year. We see lower NO_x emissions in February 2020.

2.3 In-situ observations

More than 1500 in-situ stations covering all major cities in China are operated by the China National Environmental Monitoring Centre. They provide hourly observations of the pollutants PM_{10}, $PM_{2.5}$, O_3, NO_2, SO_2, and CO (Bai et al., 2020). NO_2 is measured by a chemiluminescence technique (Zhang & Zhao, 2015). Data can be accessed via web-sites of third parties, such as www.pm25.in and www.aqicn.org. For this study we have averaged the various in-situ NO_2 observations in a city to a single value per hour for each of 36 selected major cities. For comparison with model results, we calculated a daily value based on the observations from 10:00 to 18:00 local time. The daytime selection is due to large inaccuracies in simulations of the nighttime boundary layer height.

2.4 Ensemble modelling

An operational multi-model forecasting system for air quality has been developed to provide air quality services for urban areas of China (Brasseur et al., 2019, Petersen et al., 2019). This system has been developed within the EU-funded FP-7 projects: MarcoPolo and PANDA. The ensemble model system includes nine global and regional chemistry-transport models from different research institutes from Europe and China. The ensemble service has a typical resolution of about 20 km. It provides daily forecasts of ozone, nitrogen oxides, and particulate matter for the 36 largest urban areas of East China (i.e. population higher than 3 million according to the census of 2010 (NBS, 2010). These individual 3-day forecasts as well as the mean and median concentrations are publicly accessible (http://www.marcopolo-panda.eu). The emission inventories used as input to the models of the ensemble do not account for the Chinese New Year or the COVID-19 lock down period. Therefore, the ensemble model represents the business-as-usual scenario.

3 NO_x emissions reductions

NO_x emissions have been affected since the strict regulations started in China, especially in Hubei. We select three periods to quantify the impact of the COVID-19 regulations. The first period (P1) is three weeks before the implementation of the COVID-19 regulations, 3 to 23 January in 2020, which is also just before the Chinese New Year. The second period (P2) is 8 to 28 February, which is regarded as the regulation period. The third period (P3) is from 18 March to 7 April, when most regions in China resumed working. We calculated the average of NO_x emissions derived with DECSO in each period and compare their differences. Figure 2 shows the relative changes of NO_x emissions during the selected 3 periods over the grid cells with high anthropogenic (above 3kg N/km^2/day) NO_x emissions. We observe a strong decrease by at least 30% of NO_x emissions over China in P2 compared to P1 (Figure S1 shows the emission changes on provincial level). A few grid cells with increased emissions often coincide with industrial areas. In P3, NO_x emissions increased compared to P2 but are still lower than in P1 because of the step-wise resumption of work and social life. The NO_x emissions in South Korea are not significantly changed in P2 compared to the changes in China during the three periods (Figure S1), because South Korea adopted less restrictive COVID-19 regulations, mostly on voluntary basis (Bauwens et al., 2020). In Figure 2, we see that the NO_x emissions over sea also decrease. We calculate the NO_x emissions over the ship lanes over Chinese seas defined in the study of Ding et al. (2018). The emissions due to sea-transport from Shanghai to Guangzhou are less affected than the transport over landand are found to decrease by about 25% in P2 and increase again with 18% in P3 in comparison to P2. A more significant emission decline was found in the Yellow Sea and Bohai area, where NO_x emissions reduced by about 41% in P2 and continued decreasing by 6% in P3.

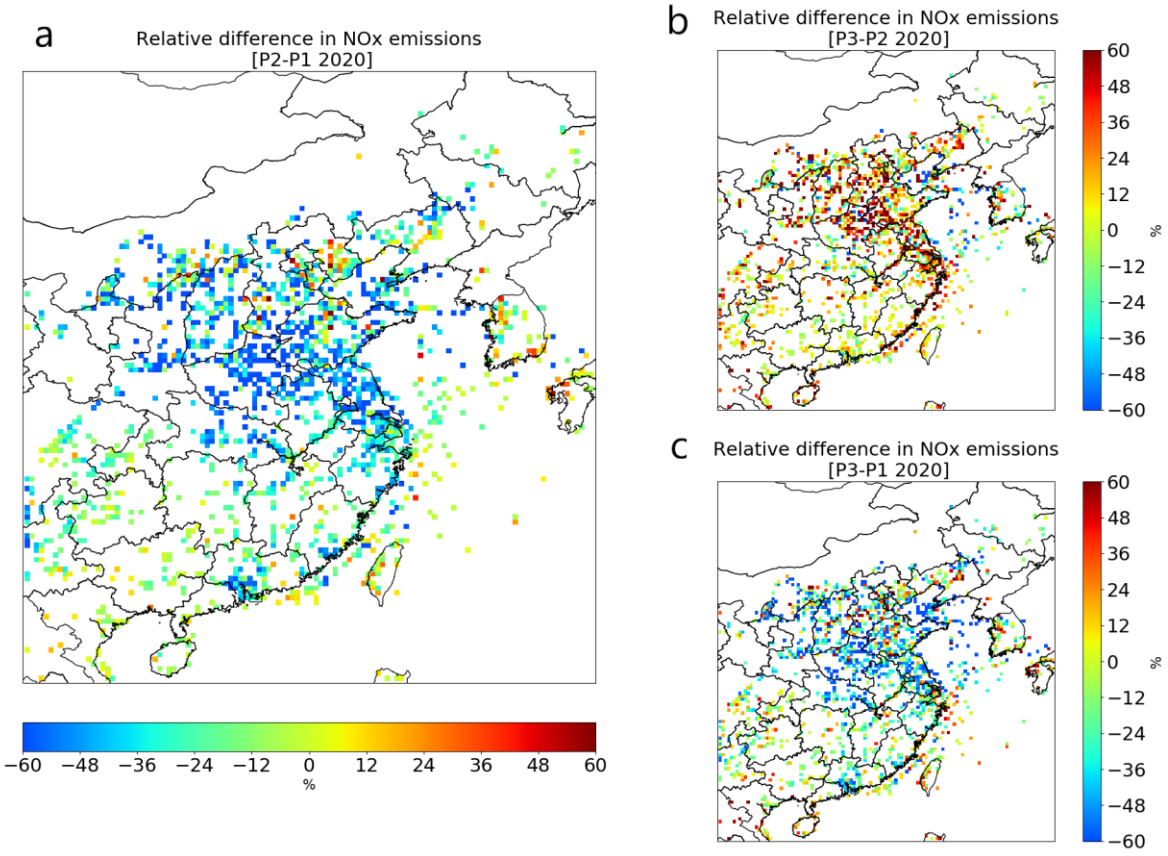

Figure 2. The relative difference in NOx emissions between (a) P2 and P1; (b) P3 and P2 (c) P3 and P1. P1 is 3-23 January. P2 is 8-28 February. P3 is 18 March to 7 April. The changes in emissions are shown in the figure for emissions higher than 3 kg(N)/km^2/day in P1 to remove areas with dominating biogenic emissions or rural areas.

At city level changes in NO_x emissions started from January 2019. Figure 3 shows the time series of emissions at 6 large cities in China and in Seoul, the capital of South Korea. We infer a very strong NO_x emission decrease of more than 50% during and after the 2020 Chinese New Year in Wuhan, where the COVID-19 outbreak was first recorded and very strict lockdown regulations were adopted. At the other five Chinese cities, we also observe a much stronger decrease after the Chinese New Year in 2020 than in 2019. In addition, the duration of the period with low emissions is much longer. Most cities in China display a stronger decrease in 2020 (see Table S1), which is attributed to the COVID-19 measures. The averaged NO_x emission reduction at the selected cities shown in table S1 is 35%. We also calculate the average reduction of grid cells containing urban areas selected by using the land-use data of the GlobCover Land Cover dataset, which was implemented in the CTM by Ding et al. (2015). The inferred emission reduction is about 35% in urban areas, which is the same as the average reduction in the selected cities. Note that the NO_x emissions are usually lower by about 10% during the Chinese New Year with less business and industrial activities (Ding et al., 2017). The time line of NO_x emissions in Beijing show a slightly different pattern with a relatively low reduction during the COVID-19 lockdown, but already strong emission reductions during the politically important

"two-sessions" meeting in March 2019, the most important political meeting of China, and especially the celebration of 70th national anniversary of China around 1 October 2019, when many factories were closed and strict emission regulations were enforced (Yang et al., 2020). Figure 3 also shows that the NO_x emissions start to increase again in March, in line with the step-by-step recovery of the human activities. Except for Wuhan with the emission rebound after 8 April, when the lockdown was lifted, by the end of March all cities reached a level of NO_x emissions close to what was observed in the same period in 2019. This is consistent with the economic target of China that they will accelerate the return to the pre-crisis economic level after the temporary economic setback due to the COVID-19 outbreak as was reported by Ouyang (2020)

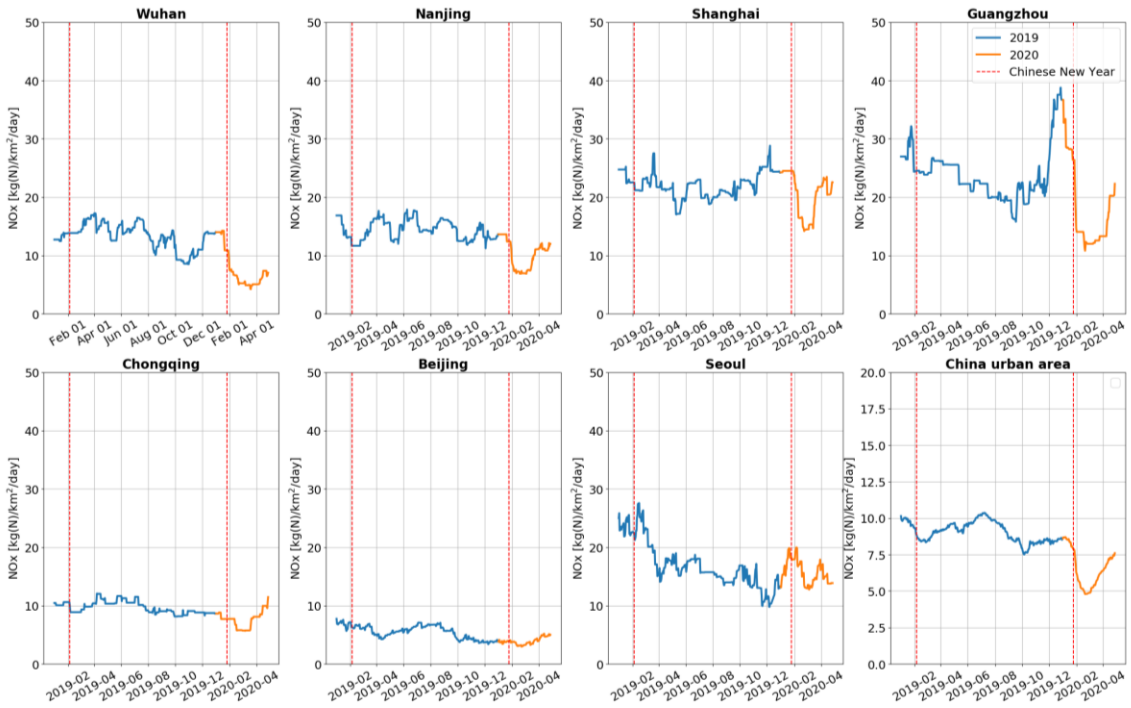

Figure 3. Time series (1 January 2019 to 28 April 2020) of daily NO_x emissions in 7 cities and urban China. 6 Chinese cities are considered (Wuhan, Nanjing, Shanghai, Guangzhou, Chongqing and Beijing) as well as Seoul. The location of Chinese cities is shown in Figure S4.

Besides the urban emissions, we find strong reductions of NO_x emissions from coal power plants. Figure 4 shows time series of NO_x emissions from the Ningxia Province, where the main sources of NO_x are fossil fuel power plants (van der A et al., 2017). Ningxia province can serve as an indication of the national energy production by coal power plants. It has a population of about 6 million, only 0.4% of the total population of China. Its coal production and electricity generation from coal power plants are in the top ten list of provinces and about 80% of the generated energy is consumed by the industry (Ningxia Statistics Bureau, 2019). Our inversion

results indicate that after the 2020 Chinese New Year, NO_x emissions dropped about 40% in this province, 20% more than in 2019 New Year period. This shows the impact of the COVID-19 regulations on the energy production, especially in the industrial sector. According to the National Bureau of Statistics of China (2020), the total profit of the first three months in 2020 made by industrial enterprises decreased around 40% in China compared to the same period of the previous year. The shrinking of the industrial economy results in lower energy consumption, which is clearly reflected by the decrease of NO_x emissions from power plants.

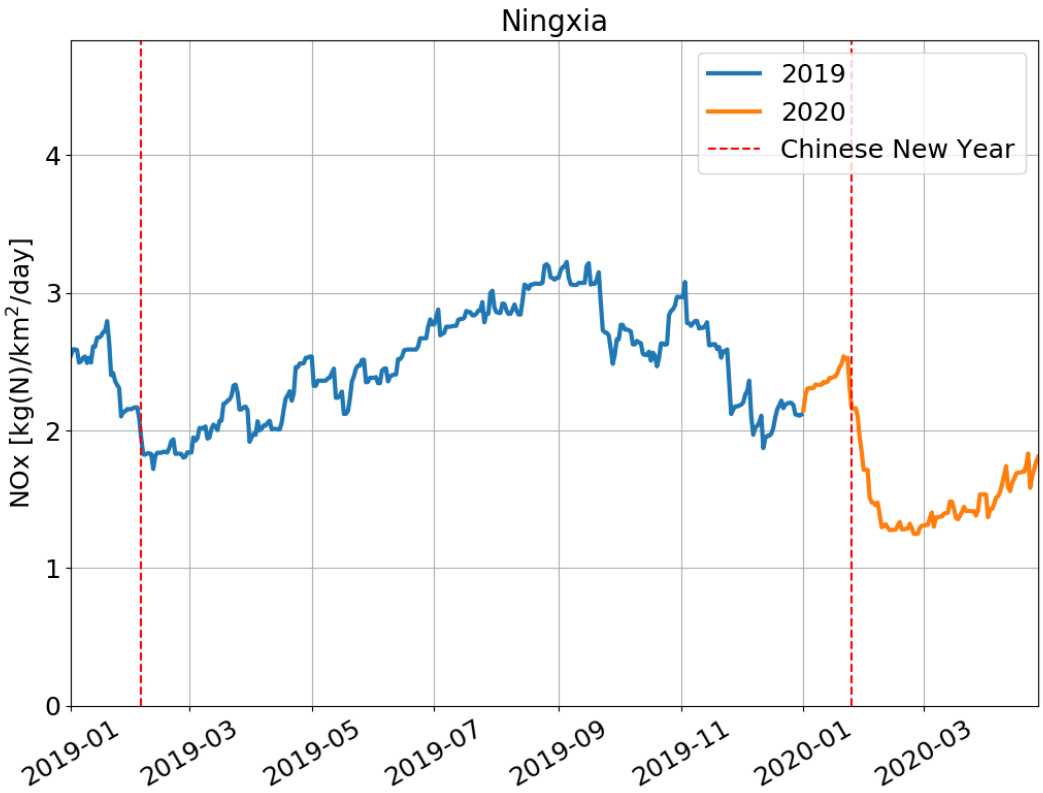

Figure 4. Time series (1 January 2019 to 28 April 2020) of daily NOx emissions in Ningxia Province.

4 Surface concentration reductions

The effect of the emission reductions on the surface concentration is very relevant for air pollution. In Figure S2 we show the emissions and the modelled surface concentrations from DECSO based on these emissions. Although we see a similar time course in both, the reductions in emissions and surface concentrations are different due to the changing meteorology and lifetime of NO_x over time. To further verify the reductions in surface concentrations we used measurements of the in-situ stations described in section 2.3. To eliminate the effect of meteorology and transport we compare the measurements of in-situ stations with the ensemble model introduced in section 2.4. The model is driven by emission inventories, which are not

corrected for the effects of either Spring Festival or the COVID-19 crisis and hence are considered the business-as-usual situation. A possible bias between measurements and model is corrected for by normalizing the results for the first two weeks of January. In Figure 5 the ratio between in-situ measured NO_2 and the modelled NO_2 is shown. The concentration reductions are shown as green area, while increased concentrations are shown in red. The reduction starts around the Chinese New Year and ends in March. Exception is the concentration level of Wuhan that becomes similar to that of the business-as-usual scenario after the first week of April. Table S1 shows the concentration reduction in P2 compared to P1 for the selected 36 cities. The average concentration reduction is 41%, while for emissions the reduction is 35%. A striking difference between Wuhan and the other Chinese cities is the longer duration (by about one month) of the concentration reductions.

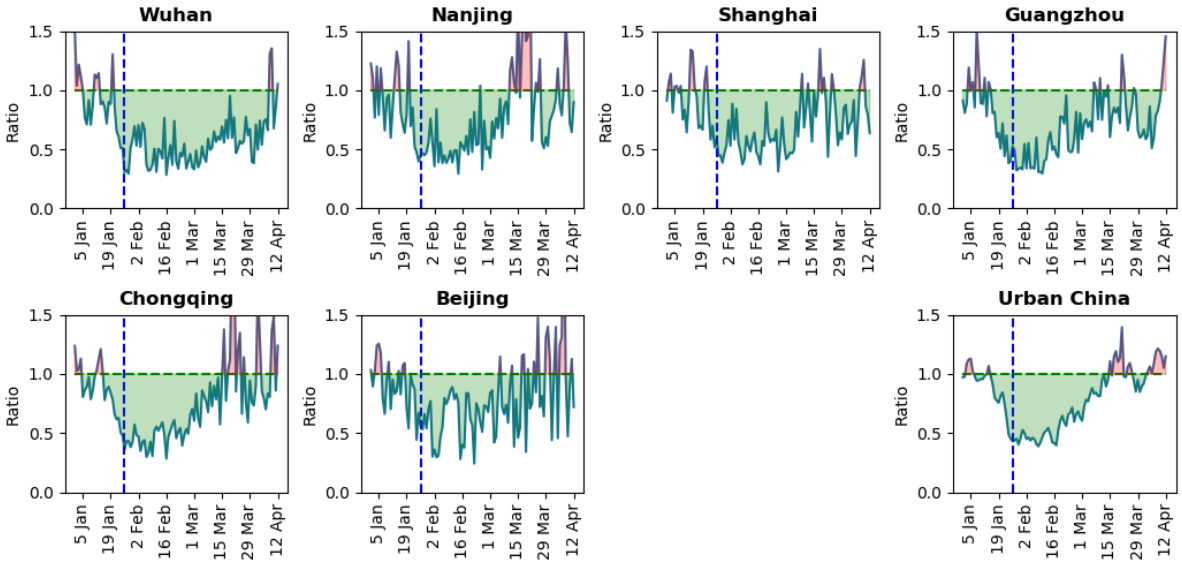

Figure 5. Measured NO_2 concentrations (from 1 January to 12 April 2020) compared to concentrations of the business-as-usual scenario. Cities are chosen similar to Figure 3, except for Seoul. The Chinese New Year is indicated by the blue dashed line.

5 Conclusions

To study the impact of the COVID-19 regulations on NO_x emissions (one of the key ingredients determining air pollution), we derived daily NO_x emissions at a resolution of 0.25° × 0.25° over East Asia from 2019 to March 2020 by applying the inverse algorithm DECSO to observations from TROPOMI. By grouping the emission into three periods of before, during and after the COVID-19 regulations, we quantified the emission changes on the small spatial scale of city level and from different emission sources such as sea-transport and the energy sector. The observations suggest emission reductions of 20% to 50% for cities. The emissions reduction of 40% in the Ningxia province reflects the impact of the lockdown measures on the energy sector. Maritime transport is also affected during the COVID-19 regulations, although its emissions reductions are dependent on the region. Along the ship track from Shanghai to Guangzhou, the NO_x emissions decreased by 25% during the lockdown and increased again by 18% after the work resumption. While in the region of the Yellow sea and Bohai sea, the emissions decrease

by 40% and continued decreasing with another 6% also in March. To further assess the impact of emission reductions, we compared the in situ NO_2 concentration measurements with simulated surface concentrations from models using unaltered emissions. The emission reductions follow a similar timeline as the surface NO_2 concentrations, which show a sharp reduction around the Chinese New Year and a slow recovery from mid-February to mid-March. Wuhan, the city of the epicenter of the COVID-19 crisis, shows large emission reductions in both February and March, reaching nominal levels in April. In general, we found that activities in the cities returned to normal in March, while as an indicator of the economy, emissions of energy production and international maritime transport, took a longer time to return to pre-COVID-19 levels (Table S2).

With the NO_x emissions derived from DECSO using observations from TROPOMI, we are able to get detailed information about the impact on emission changes due to the COVID-19 regulations by accounting for the influence of meteorology, lifetime and transport of the air pollutants. As the COVID-19 crisis progressively affects all continents, the public health regulations implemented by various countries may have different contributions to air quality. Applying our methodology to different regions can help to quantify the impact of the NO_x emission reductions by the different regulations on not only the improvement of air quality from urban to local to regional scale.

Acknowledgments and Data

This research has been supported by the project “Impact study of COVID-19 lockdown measures on air quality and climate” of the European Space Agency (grant number 4000127610/19/I-NS). This publication contains modified Copernicus Sentinel-5P data 2019-2020. TROPOMI data are available at http://www.temis.nl/airpollution/no2col/tropomi_data.php. We acknowledge the ESA GlobCover project for the land use data set on http://due.esrin.esa.int/page_globcover.php. The NO_x emissions dataset in this study is available on http://www.globemission.eu/region_asia/datapage.php?species=NOx_TROPOMI.

References

Bai, K., Li, K, Guo, J., Yang, Y., Chang, N.-B. (2020). Filling the gaps of in situ hourly PM2.5 concentration data with the aid of empirical orthogonal function analysis constrained by diurnal cycles. *Atmospheric Measurement Techniques*, 13, 3, 1213-1226, DOI: 10.5194/amt-13-1213-2020.

Bauwens, M., Compernolle, S., Stavrakou, T., Müller, J.-F., van Gent, J., Eskes, H.,et al. (2020). Impact of coronavirus outbreak on NO_2 pollution assessed using TROPOMI and OMI observations. *Geophysical Research Letters*, https://doi.org/10.1029/2020GL087978,, 2020

Boersma, K. F., Vinken, G. C. M., & Eskes, H. J. (2016). Representativeness errors in comparing chemistry transport and chemistry climate models with satellite UV–Vis tropospheric column retrievals. Geosci. Model Dev., 9(2), 875-898. doi:10.5194/gmd-9-875-2016

Brasseur, G. P., Xie, Y., Petersen, A. K., Bouarar, I., Flemming, J., Gauss, M., et al. (2019). Ensemble forecasts of air quality in eastern China - Part 1: Model description and implementation of the MarcoPolo-Panda prediction system, version 1, *Geosci. Model Dev*., 12, 33-67, https://doi.org/10.5194/gmd-12-33-2019.

Ding, J., van der A, R. J., Mijling, B., Levelt, P. F., & Hao, N. (2015). NOx emission estimates during the 2014 Youth Olympic Games in Nanjing. *Atmos. Chem. Phys*., 15(16), 9399-9412. doi:10.5194/acp-15-9399-2015

Ding, J., Miyazaki, K., van der A, R. J., Mijling, B., Kurokawa, J. I., et al. (2017). Intercomparison of NOx emission inventories over East Asia. *Atmos. Chem. Phys.*, 17(16), 10125-10141. doi:10.5194/acp-17-10125-2017

Ding, J., A, R. J., Mijling, B., Jalkanen, J. P., Johansson, L., & Levelt, P. F. (2018). Maritime NOx Emissions Over Chinese Seas Derived From Satellite Observations. Geophysical Research Letters, 45(4), 2031-2037. doi:doi:10.1002/2017GL076788

Goldberg, D., L., Lu, Z., Streets, D., G., de Foy, B., Griffin, D., McLinden, C., A., et al. (2019). Enhanced Capabilities of TROPOMI NO2: Estimating NOX from North American Cities and Power Plants, *Environ. Sci. Technol*., 53, 21, 12594-12601, https://doi.org/10.1021/acs.est.9b04488.

Gu, J., Chen, L., Yu, C., Li, S., Tao, J., Fan, M., et al. (2017) Ground-Level NO2 Concentrations over China Inferred from the Satellite OMI and CMAQ Model Simulations. *Remote Sens*., 9(6), 519, https://doi.org/10.3390/rs9060519

Huang, X., Ding, A., Gao, J., Zheng, B., Zhou, D., et al. (2020). Enhanced secondary pollution offset reduction of primary emissions during COVID-19 lockdown in China. *EarthArXiv*., April 13. https://doi.org/10.31223/osf.io/hvuzy

Judd, L. M., Al-Saadi, J. A., Szykman, J. J., Valin, L. C., Janz, S. J., Kowalewski, M. G., et al. (2020). Evaluating Sentinel-5P TROPOMI tropospheric NO2 column densities with airborne and Pandora spectrometers near New York City and Long Island Sound. Atmos. Meas. Tech. Discuss., 2020, 1-52. doi:10.5194/amt-2020-151

Liu, F., Page, A., Strode, S. A., Yoshida, Y., Choi, S., Zheng, B., et al. (2020). Abrupt decline in tropospheric nitrogen dioxide over China after the outbreak of COVID-19. Science Advances, eabc2992. doi:10.1126/sciadv.abc2992

Menut, L., Bessagnet, B., Khvorostyanov, D., Beekmann, M., Blond, N., Colette, A., et al. (2013). CHIMERE 2013: A model for regional atmospheric composition modelling. *Geoscientific Model Development*, 6(4), 981–1028. https://doi.org/10.5194/gmd-6-981-2013

Mijling, B., and van der A, R. J. (2012). Using daily satellite observations to estimate emissions of short-lived air pollutants on a mesoscopic scale. *Journal of Geophysical Research: Atmospheres*, 117(D17). doi:10.1029/2012JD017817

Miyazaki, K., Eskes, H. J., & Sudo, K. (2012). Global NOx emission estimates derived from an assimilation of OMI tropospheric NO2 columns. Atmospheric Chemistry and Physics, 12(5), 2263-2288. doi:10.5194/acp-12-2263-2012

Miyazaki, K., Bowman, K., Sekiya, T., Eskes, H., Boersma, F., Worden, H., et al. (2020). An updated tropospheric chemistry reanalysis and emission estimates, TCR-2, for 2005–2018, *Earth Syst. Sci. Data Discuss.*, https://doi.org/10.5194/essd-2020-30, in review.

National Bureau of Statistics of China (2020). Available online: http://www.stats.gov.cn/english/PressRelease/202004/t20200428_1742015.html (last access date: 3 May 2020)

NBS, National Bureau of Statistics, China Statistical Yearbook 2010 ,Beijing: China Statistics Press, 2010

Ningxia Statistics Bureau (2019). The Achivements of Economic and Social Development during the last 70 years, part 3, in Chinese. Available online: http://tj.nx.gov.cn/tjxx/201909/t20190923_1750612.html (last access date: 9 May 2020)

Ouyang S. (2020). COVID-19 will not alter China's growth story, top economic regulator says, *China Daily*. Available online: https://global.chinadaily.com.cn/a/202004/20/WS5e9d51f8a3105d50a3d1779c.html (last access date: 27 April 2020)

Petersen, A. K., Brasseur, G. P., Bouarar, I., Flemming, J., Gauss, M., Jiang, F., et al (2019). Ensemble forecasts of air quality in eastern China - Part 2: Evaluation of the MarcoPolo-Panda prediction system, version 1. *Geosci. Model Dev.*. 12, 1241-1266, https://doi.org/10.5194/gmd-12-1241-2019.

Shindell, D. T., Faluvegi, G., Koch, D. M., Schmidt, G. A., Unger, N., & Bauer, S. E. (2009). Improved Attribution of Climate Forcing to Emissions. *Science*. 326(5953), 716-718. doi:10.1126/science.1174760

Stavrakou, T., Müller, J.-F., Boersma, K. F., van der A, R. J., Kurokawa, J., Ohara, T., and Zhang, Q. (2013). Key chemical NO_x sink uncertainties and how they influence top-down emissions of nitrogen oxides, *Atmos. Chem. Phys.*, 13, 9057–9082, https://doi.org/10.5194/acp-13-9057-2013,.

Tack, F., Merlaud, A., Iordache, M. D., Pinardi, G., Dimitropoulou, E., Eskes, H., et al. (2020). Assessment of the TROPOMI tropospheric NO2 product based on airborne APEX observations. Atmos. Meas. Tech. Discuss., 2020, 1-55. doi:10.5194/amt-2020-148

Tian, H., Liu, Y., Li, Y., Wu, C.-H., Chen, B., Kraemer, M. U. G., et al. (2020). An investigation of transmission control measures during the first 50 days of the COVID-19 epidemic in China. *Science*, eabb6105. doi:10.1126/science.abb6105

van der A, R. J., Mijling, B., Ding, J., Koukouli, M. E., Liu, F., Li, Q., et al. (2017). Cleaning up the air: effectiveness of air quality policy for SO_2 and NO_x emissions in China. *Atmos. Chem. Phys.*, 17(3), 1775-1789. doi:10.5194/acp-17-1775-2017

van der A, R. J., de Laat, A. T. J., Ding, J., & Eskes, H. J. (2020). Connecting the dots: NO_x emissions along a West Siberian natural gas pipeline. *npj Climate and Atmospheric Science*, 3(1), 16. doi:10.1038/s41612-020-0119-z

van Geffen, J., Boersma, K. F., Eskes, H., Sneep, M., ter Linden, M., Zara, M., and Veefkind, J. P.: S5P TROPOMI NO_2 slant column retrieval: method, stability, uncertainties and comparisons with OMI, *Atmos. Meas. Tech.*, 13, 1315–1335, https://doi.org/10.5194/amt- 13-1315-2020, 2020.

van Geffen, J. H. G. M., Eskes, H. J., Boersma, K. F., Maasakkers, J. D., and Veefkind, J. P. (2019). TROPOMI ATBD of the total and tropospheric NO_2 data products, Report S5P-KNMI-L2-0005-RP, version 1.4.0, released 6 February 2019, KNMI, De Bilt, the Netherlands, available at: http://www.tropomi.eu/documents/atbd/, last access: 17 March 2020.

Veefkind, J. P., Aben, I., McMullan, K., Förster, H., de Vries, J., Otter, G., et. al. (2012). TROPOMI on the ESA Sentinel-5 Precursor: A GMES mission for global observations of the atmospheric composition for climate, air quality and ozone layer applications. *Remote Sensing of Environment*, 120, 70-83. doi:https://doi.org/10.1016/j.rse.2011.09.027

Verhoelst, T., Compernolle, S., Pinardi, G., Lambert, J. C., Eskes, H. J., Eichmann, K. U., et al. (2020). Ground-based validation of the Copernicus Sentinel-5p TROPOMI NO2 measurements with the NDACC ZSL-DOAS, MAX-DOAS and Pandonia global networks. Atmos. Meas. Tech. Discuss., 2020, 1-40. doi:10.5194/amt-2020-119

Wang, P., Chen, K., Zhu, S., Wang, P., & Zhang, H. (2020). Severe air pollution events not avoided by reduced anthropogenic activities during COVID-19 outbreak. *Resources, Conservation and Recycling*, 158, 104814. doi:https://doi.org/10.1016/j.resconrec.2020.104814

WHO (2020). The World Health Organization. Coronavirus Disease (COVID-19) Pandemic. Available online: https://www.who.int/emergencies/diseases/novel-coronavirus-2019 (last access date: 27 April 2020)

Yang, Y., Wang, Y., Yao, D., Zhao, S., Yang, S., et al. (2020). Significant decreases in the volatile organic compound concentration, atmospheric oxidation capacity and photochemical reactivity during the National Day holiday over a suburban site in the North China Plain, *Environmental Pollution*, Volume 263, Part A, 114657, https://doi.org/10.1016/j.envpol.2020.114657.

Zhang, R., Zhang, Y., Lin, H., Feng, X., Fu, T.-M., & Wang, Y. (2020). NO_x Emission Reduction and Recovery during COVID-19 in East China. *Atmosphere*, *11*(4), 433

Zhang, Y., Cao, F. (2015) Fine particulate matter (PM2.5) in China at a city level. Sci Rep 5, 14884. https://doi.org/10.1038/srep14884

Figure 1.

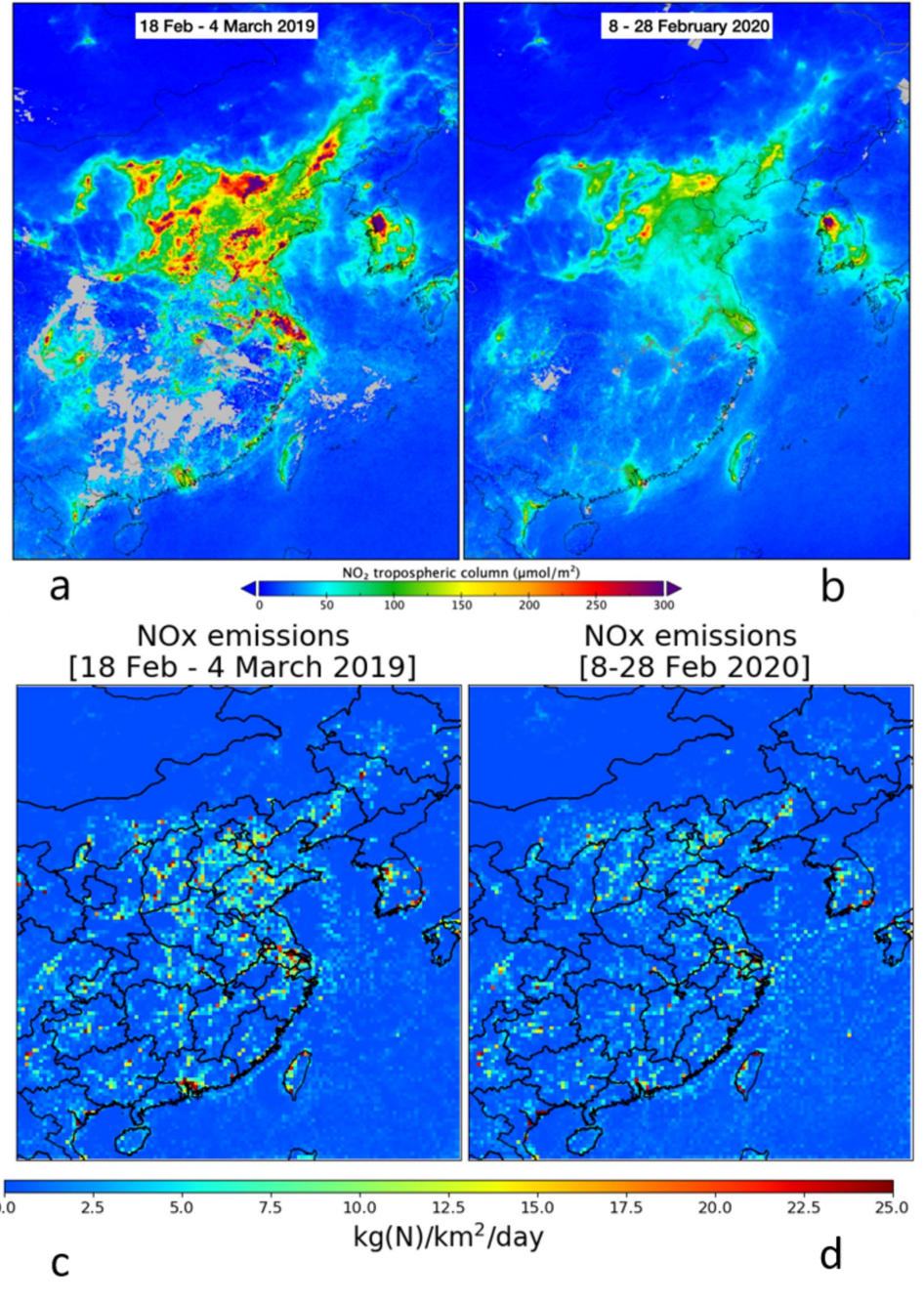
18 Feb - 4 March 2019
8 - 28 February 2020
a
NO_2 tropospheric column (μmol/m²)
0
50
100
150
200
250
300
b
NOx emissions
[18 Feb - 4 March 2019]
NOx emissions
[8-28 Feb 2020]
0.0
2.5
5.0
7.5
10.0
12.5
15.0
17.5
20.0
22.5
25.0
kg(N)/km²/day
c
d

Figure 2.

a

Relative difference in NOx emissions
[P2-P1 2020]

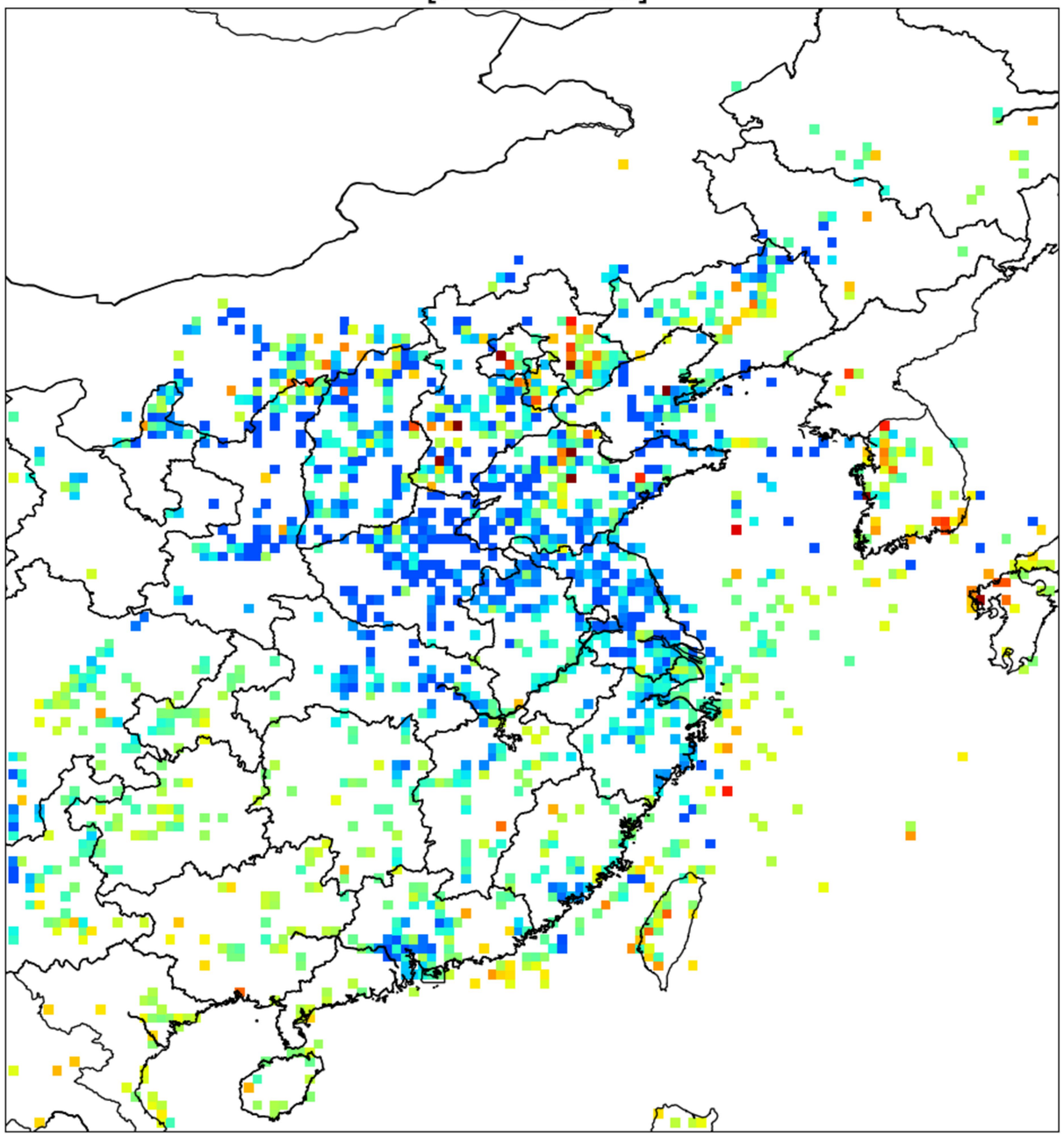

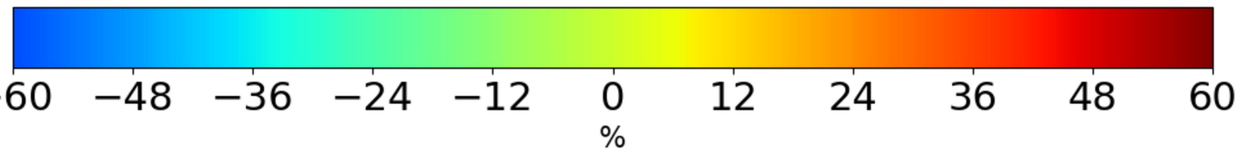

b

Relative difference in NOx emissions
[P3-P2 2020]

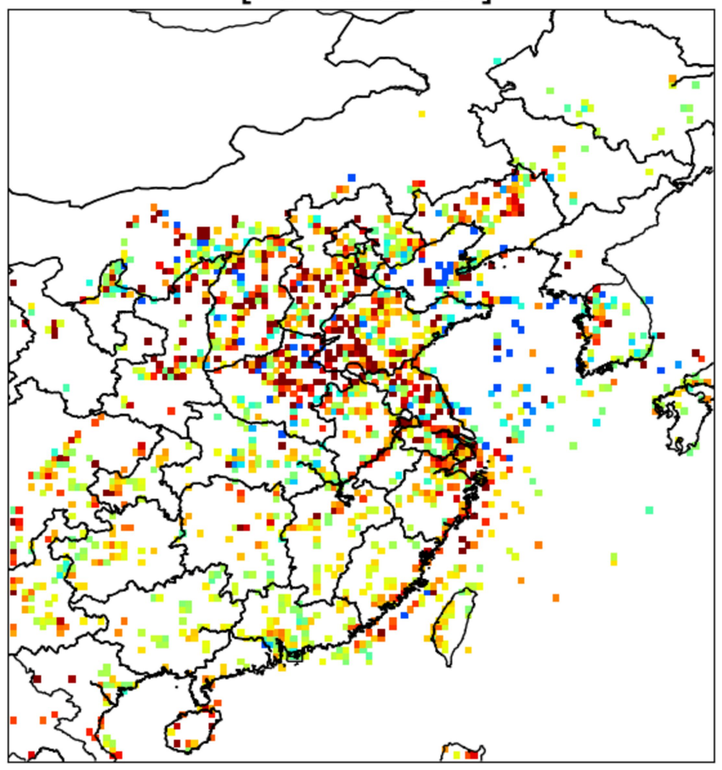

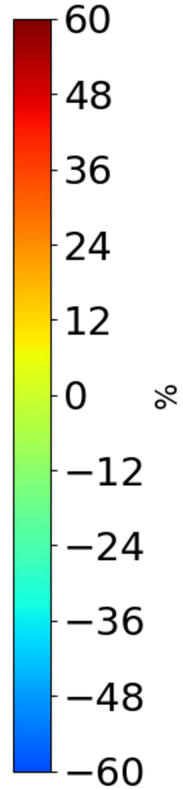

C

Relative difference in NOx emissions
[P3-P1 2020]

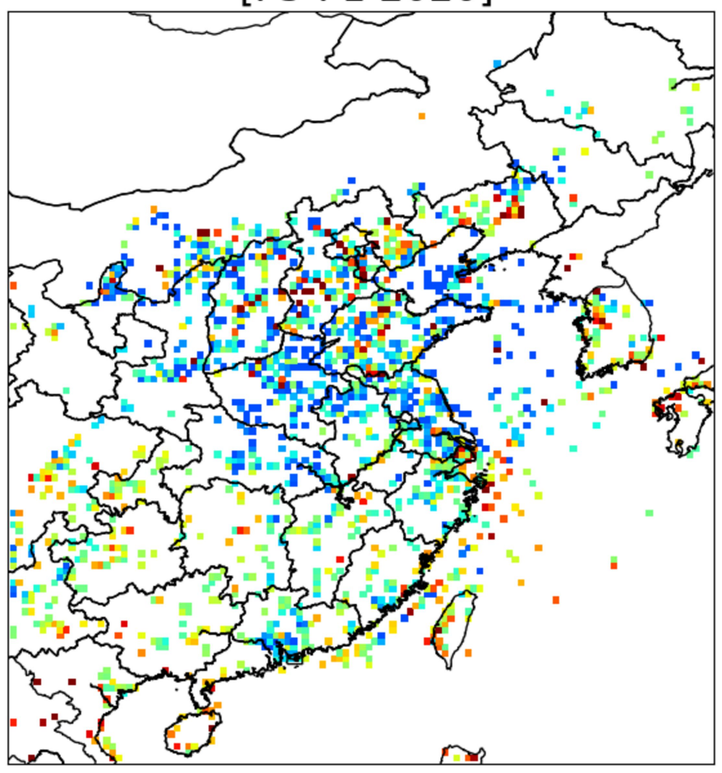

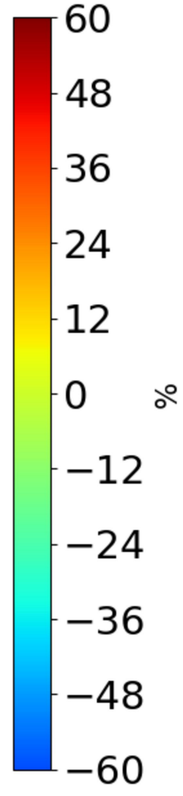

Figure 3.

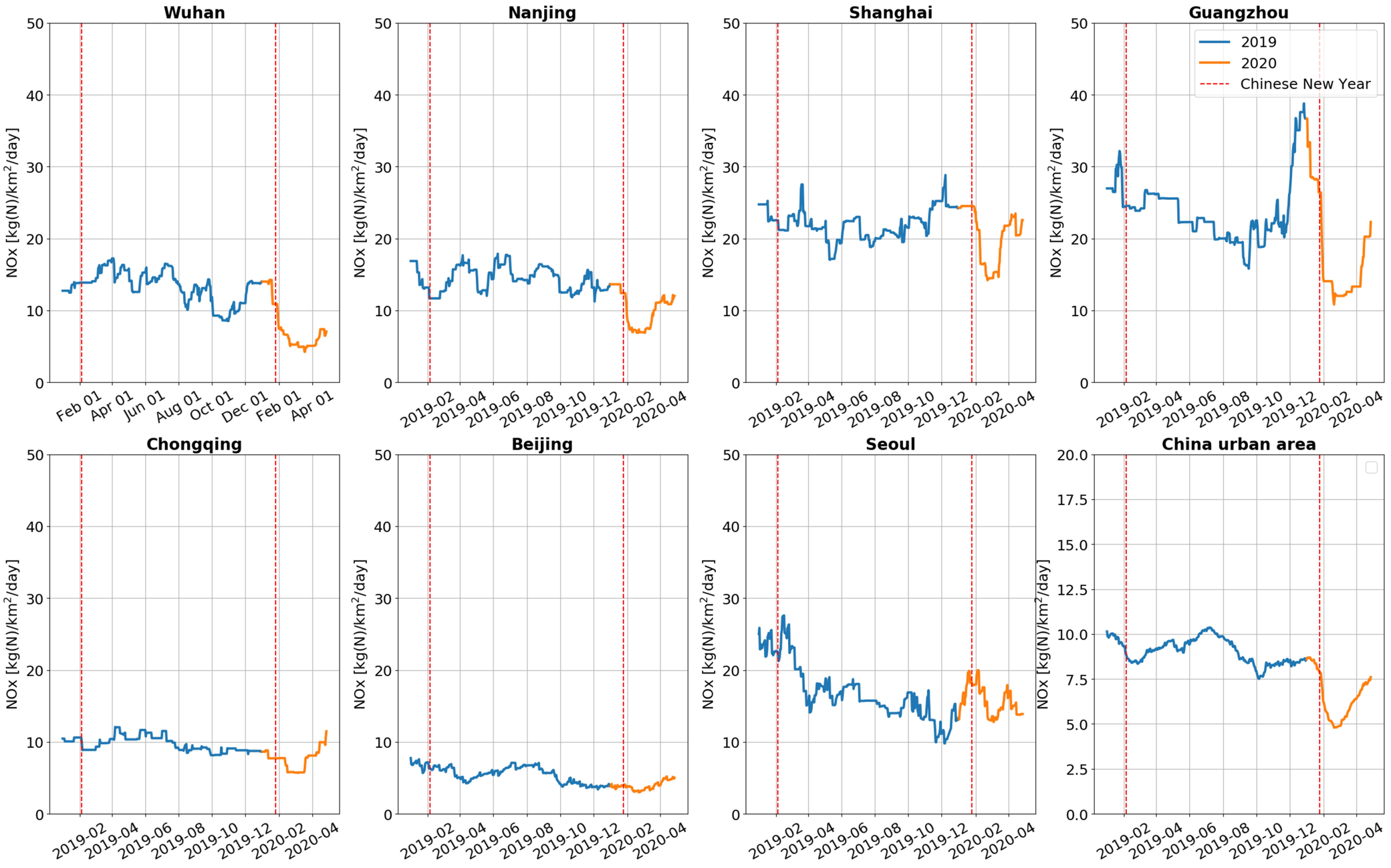
Wuhan
Nanjing
Shanghai
Guangzhou
Chongqing
Beijing
Seoul
China urban area
NOx [kg(N)/km^2/day]
2019
2020
Chinese New Year
Feb 01
Apr 01
Jun 01
Aug 01
Oct 01
Dec 01
2019-02
2019-04
2019-06
2019-08
2019-10
2019-12
2020-02
2020-04

Figure 4.

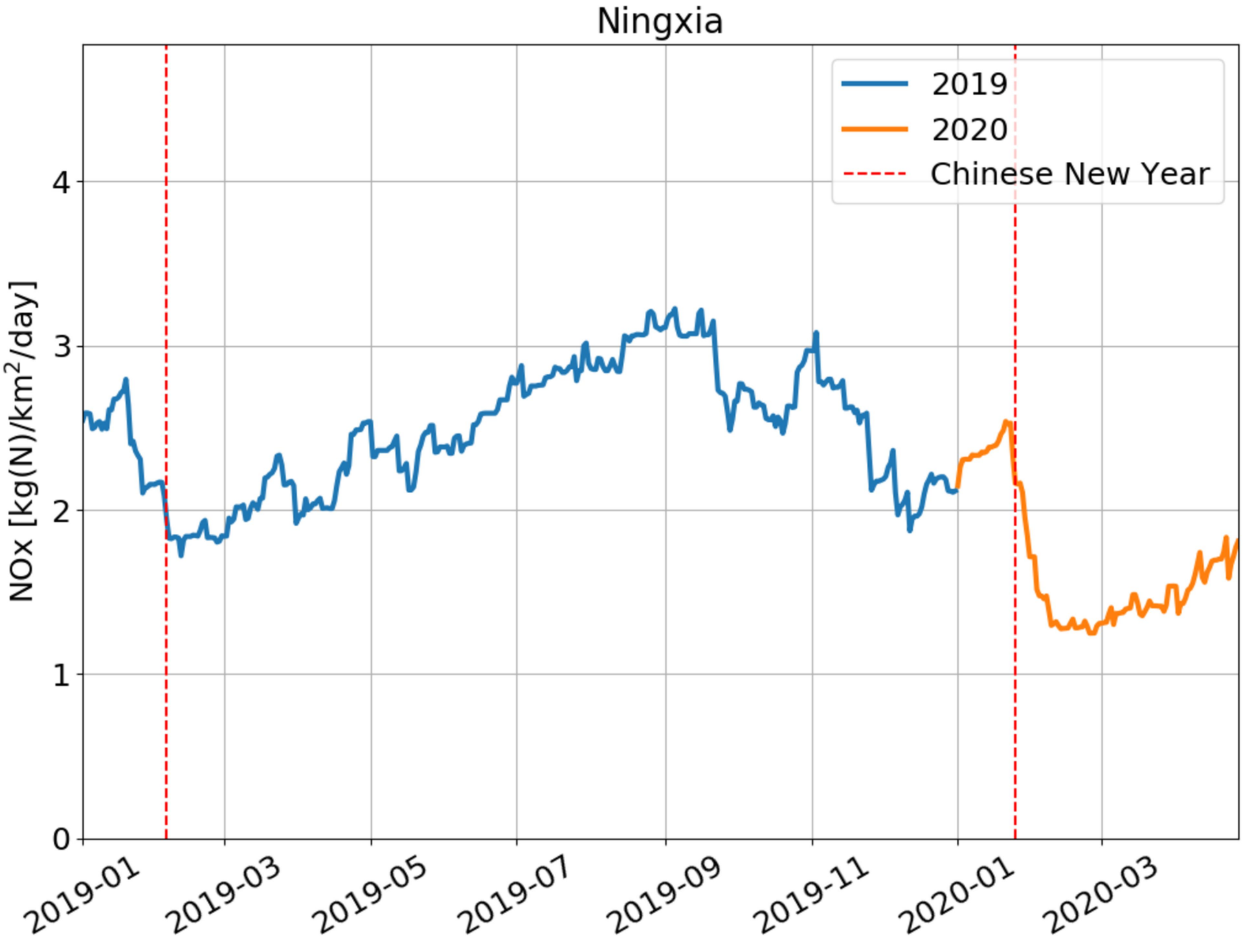
Ningxia
2019
2020
Chinese New Year
NOx [kg(N)/km^2/day]
0
1
2
3
4
2019-01
2019-03
2019-05
2019-07
2019-09
2019-11
2020-01
2020-03

Figure 5.

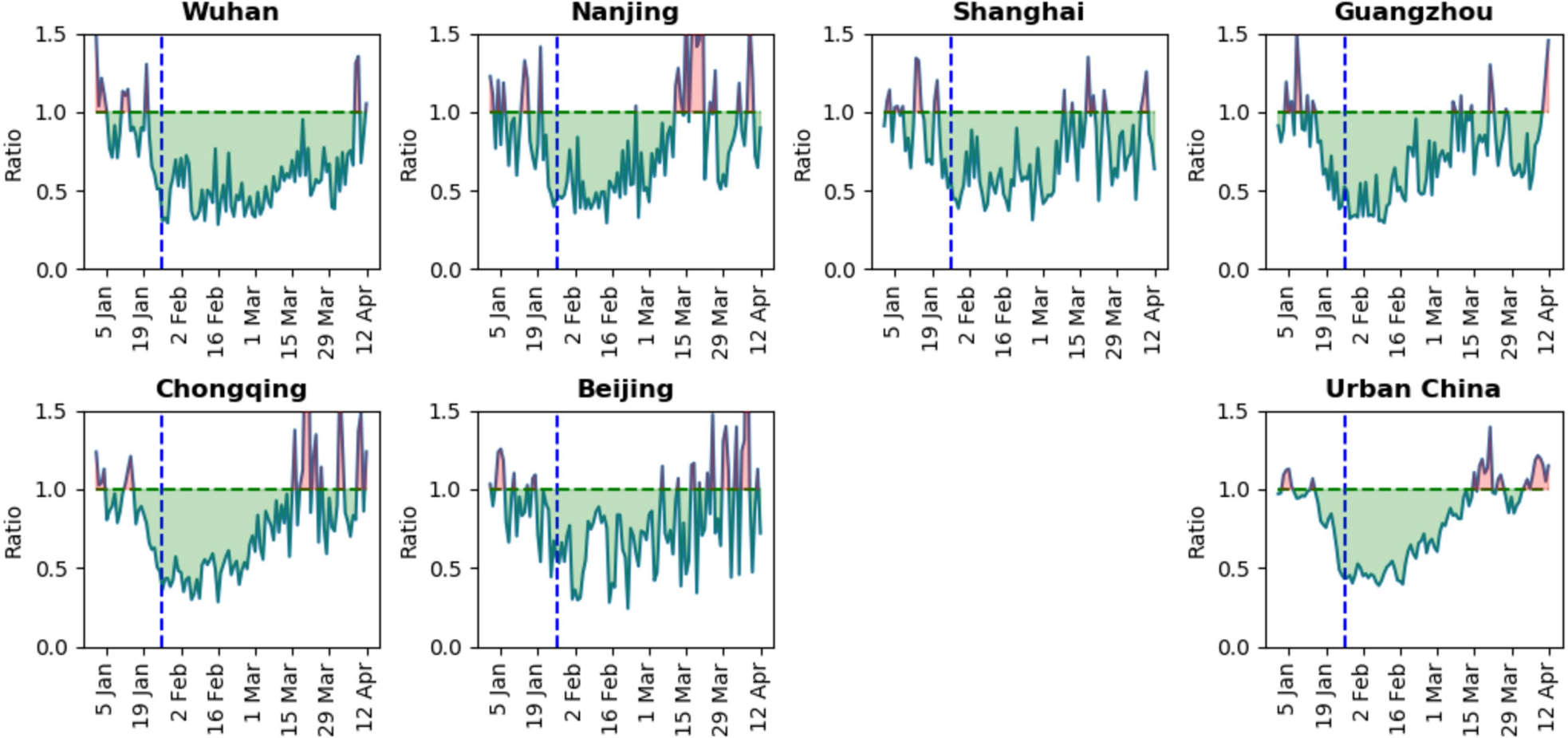
Wuhan
Nanjing
Shanghai
Guangzhou
Chongqing
Beijing
Urban China
Ratio
1.5
1.0
0.5
0.0
5 Jan
19 Jan
2 Feb
16 Feb
1 Mar
15 Mar
29 Mar
12 Apr